

# EXAFS and XRD studies of an amorphous $\text{Co}_{57}\text{Ti}_{43}$ alloy produced by mechanical alloying

K. D. Machado,\* J. C. de Lima, C. E. M. Campos, T. A. Grandi, and A. A. M. Gasperini  
*Departamento de Física, Universidade Federal de Santa Catarina, 88040-900 Florianópolis, SC, Brazil*  
(Dated: November 12, 2018)

We have investigated the local atomic structure of an amorphous  $\text{Co}_{57}\text{Ti}_{43}$  alloy produced by Mechanical Alloying by means of x-ray diffraction and EXAFS analyses on Co and Ti K-edges. Coordination numbers and interatomic distances were found and compared with those determined using an additive hard sphere (AHS) model associated with a  $\text{RDF}(r)$  deconvolution, and also with data from bcc- $\text{Co}_2\text{Ti}$  compound. The EXAFS results obtained indicated a shortening in the Co-Ti and Ti-Ti distances when compared to those found by the AHS-RDF method and an increase in the Co-Co and Ti-Ti distances and a large shortening in the Co-Ti one when compared to the distances found in the bcc- $\text{Co}_2\text{Ti}$  compound. In spite of these differences, coordination numbers obtained from EXAFS and AHS-RDF are similar to each other and also to those found in bcc- $\text{Co}_2\text{Ti}$ .

## I. INTRODUCTION

Mechanical alloying (MA) technique [1] is an efficient means for synthesizing crystalline and amorphous materials, as well as stable and metastable solid solutions [2, 3, 4, 5, 6, 7]. MA has also been used to produce materials with nanometer sized grains and alloys whose components have large differences in their melting temperatures and are thus difficult to produce using techniques based on melting. The few thermodynamics restrictions on the alloy composition open up a wide range of possibilities for property combinations even for immiscible elements [8]. Since temperatures reached in MA are usually very low, this low temperature process reduces reaction kinetics, allowing the production of poorly crystallized or amorphous materials. Recently, we have used MA to produce amorphous  $\text{Ni}_{60}\text{Ti}_{40}$  [3] and partially amorphous  $\text{Fe}_{60}\text{Ti}_{40}$  [9] alloys. Ni-Ti alloys are biocompatible and can be used to produce shape memory materials, and Fe-Ti alloys can be used as hydrogen storage materials. It is known that various cobalt-rich Co-TM (TM = transition metals) amorphous alloys obtained by sputtering can provide good soft magnetic characteristics, such as high saturation magnetization and low coercivity. However, sputtering produces only thin amorphous films [10], and melt-spinning has some problems in preparing amorphous ribbon and powders [11]. Thus, here we have used MA to produce an amorphous  $\text{Co}_{57}\text{Ti}_{43}$  alloy ( $a\text{-Co}_{57}\text{Ti}_{43}$ ) starting from the crystalline elemental powders. Its structural properties were studied by x-ray diffraction (XRD) and Extended X-ray absorption fine structure (EXAFS) techniques. Due to its selectivity and high sensitivity to the chemical environment around a specific type of atom of an alloy, EXAFS [12, 13, 14, 15, 16] is a technique very suitable to investigate the local atomic order of crystalline compounds and amorphous alloys. Anomalous wide angle

x-ray scattering (AWAXS) is also a selective technique, but due to the small  $K_{\text{max}}$  that can be achieved on Ti K-edge ( $\sim 4 \text{ \AA}^{-1}$ ), little information could be obtained from an AWAXS experiment on this edge. On the other hand, EXAFS measurements performed on Ti edge extended to  $\sim 15 \text{ \AA}^{-1}$ . Using this technique, we have determined coordination numbers and interatomic distances in the first coordination shell of  $a\text{-Co}_{57}\text{Ti}_{43}$ . In addition, we have modelled the atomic structure of  $a\text{-Co}_{57}\text{Ti}_{43}$  by using an additive hard sphere (AHS) model (in which the minimum distance between unlike atoms is given by  $D_{12} = (D_{11} + D_{22})/2$ , where  $D_{ij}$  is the closest approach distance between the centers of atoms  $i$  and  $j$ ), to perform the deconvolution of the radial distribution functions ( $\text{RDF}(r)$ ). The coordination numbers and interatomic distances obtained from the AHS-RDF model were compared to those found from EXAFS, and the EXAFS results obtained indicated a shortening in the Co-Ti and Ti-Ti distances when compared to those found by the AHS-RDF method. We have also compared the structural parameters of the alloy with those found in the bcc- $\text{Co}_2\text{Ti}$  compound. In spite of some differences, coordination numbers obtained from EXAFS and AHS-RDF are similar to each other and also to those found in bcc- $\text{Co}_2\text{Ti}$ .

## II. FABER-ZIMAN STRUCTURE FACTORS

According to Faber and Ziman [17], the total structure factor  $\mathcal{S}(K)$  is obtained from the scattered intensity per atom  $I_a(K)$  through

$$\mathcal{S}(K) = \frac{I_a(K) - [\langle f^2(K) \rangle - \langle f(K) \rangle^2]}{\langle f(K) \rangle^2} \quad (1)$$

$$= \sum_{i=1}^n \sum_{j=1}^n w_{ij}(K) \mathcal{S}_{ij}(K), \quad (2)$$

where  $K$  is the transferred momentum,  $\mathcal{S}_{ij}(K)$  are the

\*Electronic address: kleber@fisica.ufsc.br

partial structure factors and

$$w_{ij}(K) = \frac{c_i c_j f_i(K) f_j(K)}{\langle f(K) \rangle^2}, \quad (3)$$

and

$$\langle f^2(K) \rangle = \sum_i c_i f_i^2(K), \quad (4)$$

$$\langle f(K) \rangle^2 = \left[ \sum_i c_i f_i(K) \right]^2. \quad (5)$$

Here,  $f_i(K)$  is the atomic scattering factor and  $c_i$  is the concentration of atoms of type  $i$ . The partial and total pair distribution functions  $G_{ij}(r)$  and  $G(r)$  are related to  $S_{ij}(K)$  and  $S(K)$  through

$$G_{ij}(r) = \frac{2}{\pi} \int_0^\infty K [S_{ij}(K) - 1] \sin(Kr) dK, \quad (6)$$

$$G(r) = \frac{2}{\pi} \int_0^\infty K [S(K) - 1] \sin(Kr) dK. \quad (7)$$

From the  $G_{ij}(r)$  and  $G(r)$  functions the partial and total radial distribution functions  $\text{RDF}_{ij}(r)$  and  $\text{RDF}(r)$  can be calculated by

$$\text{RDF}_{ij}(r) = 4\pi\rho_0 c_j r^2 + rG_{ij}(r), \quad (8)$$

$$\text{RDF}(r) = 4\pi\rho_0 r^2 + rG(r), \quad (9)$$

where  $\rho_0$  is the density of the alloy (in atoms/ $\text{\AA}^3$ ). Interatomic distances are obtained from the maxima of  $G_{ij}(r)$  and coordination numbers are calculated by integrating the peaks of  $\text{RDF}_{ij}(r)$ .

### III. ADDITIVE HARD SPHERE MODEL

In the AHS model for a binary alloy, the interacting potentials between particles  $i$  and  $j$  are

$$u_{ij} = \begin{cases} 0, & r > D_{ij} \\ \infty, & r < D_{ij} \end{cases} \quad (10)$$

where  $D_{ij}$  is the closest approach distance between the centers of the particles  $i$  and  $j$ , and

$$D_{12} = \frac{D_{11} + D_{22}}{2}, \quad (11)$$

that is, the minimum approach between unlike atoms is always equal to the arithmetic mean of the diameters  $D_{11}$  and  $D_{22}$  of the two species. For this model, the Percus-Yevick (PY) equation, which can be applied to systems in which short range forces are dominant, has

an exact solution, making it possible to obtain analytical expressions for the partial pair distribution functions and partial structure factors. In 1977, Weeks [18] used the PY model to study the atomic structure of metallic glasses, assuming an isotropic and homogeneous phase that does not occur in the solid state. The extension of the PY model to study the glassy state is based on the structural characteristics of amorphous state, which can be considered as an extrapolation of the atomic structure of the liquid state. A good review of the AHS model is given in Ref. [19].

### IV. EXPERIMENTAL PROCEDURE

Blended Co (Vetec, 99.7%, particle size  $< 10 \mu\text{m}$ ) and Ti (BDH, 99.5%, particle size  $< 10 \mu\text{m}$ ) elemental powders, with nominal composition  $\text{Co}_{60}\text{Ti}_{40}$ , were sealed together with several steel balls (with diameter of about 1 cm), under an argon atmosphere, in a steel vial. The ball-to-powder weight ratio was 5:1. The vial was mounted in a high energy ball mill Spex Mixer/Mill model 8000 (working at 1200 rpm) and milled for 10 h. A ventilation system was used to keep the vial temperature close to room temperature. The composition of the as-milled powder was measured using the Energy Dispersive Spectroscopy (EDS) technique, giving a composition of 57 at. % and 43 at. % of Co and Ti, respectively, and impurity traces were not observed. XRD measurements were recorded on a Siemens diffractometer with a graphite monochromator in the diffracted beam, using the Cu  $K_\alpha$  line ( $\lambda = 1.5418 \text{\AA}$ ).  $S(K)$  was computed from the XRD patterns, after standard corrections following the procedure described by Wagner [20]. The samples for the EXAFS measurements were formed by placing the powder onto a porous membrane (Millipore,  $0.2 \mu\text{m}$  pore size) in order to achieve optimal thickness (about  $30 \mu\text{m}$ ), and neither Kapton tape nor BN were used. The EXAFS measurements were taken at room temperature in the transmission mode on the D04B beam line of LNLS (Campinas, Brazil), using a channel cut monochromator (Si 111) and two ionization chambers filled by air as detectors, working at 10% and 70% efficiency, respectively, and the beam size at the sample was about  $3 \times 1 \text{ mm}$ . This yielded a resolution of about 2.0 eV on Ti K edge and 2.5 eV on Co K edge, respectively. At these energies, harmonic rejection is irrelevant at the D04B beam line. The energy and average current of the storage ring were 1.37 GeV and 120 mA, respectively.

### V. RESULTS AND DISCUSSION

Figure 1 shows  $S(K)$  for  $a\text{-Co}_{57}\text{Ti}_{43}$ . In this figure a diffuse halo between  $K = 2.2$  and  $3.8 \text{\AA}^{-1}$  can be seen, indicating the presence of an amorphous phase. Residual crystalline peaks of the elemental metal powders are not observed. The glass-forming ability of the Co-Ti system

made by MA was investigated by Dolgin *et al* [4], Hellstern and Schultz [5] and Kimura *et al* [6]. They reported amorphization for this system, in good agreement with our results. The local atomic structure of  $\alpha$ -Co<sub>57</sub>Ti<sub>43</sub> was firstly studied considering an AHS model. We used the AHS model to obtain  $\mathcal{S}_{ij}^{\text{AHS}}(K)$  and  $G_{ij}^{\text{AHS}}(r)$  for a system with the same composition of the alloy. It is well known that the intensity of the main halo of the total structure factor  $\mathcal{S}^{\text{AHS}}(K)$  generated by the AHS model is larger than the experimental one. Thus,  $\mathcal{S}^{\text{AHS}}(K)$  has to be multiplied by a  $\exp(-\sigma^2 K^2)$  function in order to introduce a ‘thermal’ effect. The best agreement between the experimental  $G(r)$  and  $G^{\text{AHS}}(r)$  functions were achieved when the packing fraction parameter and  $\sigma^2$  values were 0.76 and 0.07 Å<sup>2</sup>, respectively. Figure 2 shows  $G(r)$  (full line) and  $G^{\text{AHS}}(r)$  (dashed line) obtained for  $\alpha$ -Co<sub>57</sub>Ti<sub>43</sub>. There is an excellent agreement concerning peak positions, in particular the first one, but there are some differences in the intensities of the peaks starting from the second one, which could be explained by the features of the AHS model. It is interesting to note that the AHS model was developed to investigate atomic structures of glassy alloys in the liquid state and, as the chemical short-range order (CSRO) of the alloy becomes stronger, it is not able to reproduce the structural features of the alloy anymore. Thus, the differences reported above can be associated with the presence of a CSRO in  $\alpha$ -Co<sub>57</sub>Ti<sub>43</sub>. This CSRO probably is not much strong since the differences between experimental and AHS data are not very large. The density of the amorphous alloy can be calculated from the slope of the straight line ( $-4\pi\rho_0 r$ ) fitting the initial part (until the first minimum) of the  $G(r)$  function [19]. We have found  $\rho_0 = \rho^{\text{AHS}} = 0.0761$  atoms/Å<sup>3</sup> for both experimental and AHS  $G(r)$  functions, whereas the average density is  $\langle \rho \rangle = c_{\text{Co}}\rho_{\text{Co}} + c_{\text{Ti}}\rho_{\text{Ti}} = 0.0763$  atoms/Å<sup>3</sup>. Figure 3 shows the experimental RDF( $r$ ) and the partial RDF $_{ij}^{\text{AHS}}(r)$  (see eq. 9) functions obtained from the AHS model. From these functions, coordination numbers and interatomic distances between first neighbors can be found, and they are given in table I. It should be noted that due to the small values of the weighting factor  $w_{\text{Ti-Ti}}(K)$  ( $w_{\text{Ti-Ti}}(K) \approx 10\%$ , see eq. 5), it is very difficult to obtain reliable structural data concerning Ti-Ti pairs using the AHS-RDF method.

The EXAFS oscillations  $\chi(k)$  at both K edges are shown in fig. 4. After standard data reduction procedures using Winxas97 software [22], they were filtered by Fourier transforming  $k^3\chi(k)$  (Co edge, 3.00 – 12.71 Å<sup>-1</sup>) and  $k\chi(k)$  (Ti edge, 3.32 – 15.00 Å<sup>-1</sup>) using a Hanning weighting function into  $r$ -space and transforming back the first coordination shells (1.30 – 2.67 Å for Co edge and 1.85 – 3.24 Å for Ti edge). Filtered spectra were then fit by using Gaussian distributions to represent the homopolar and heteropolar bonds [23]. We also used the third cumulant option of Winxas97 to investigate the presence of asymmetric shells. The amplitude and phase shifts relative to the homopolar and heteropolar bonds needed to fit them were obtained from *ab initio* calculations us-

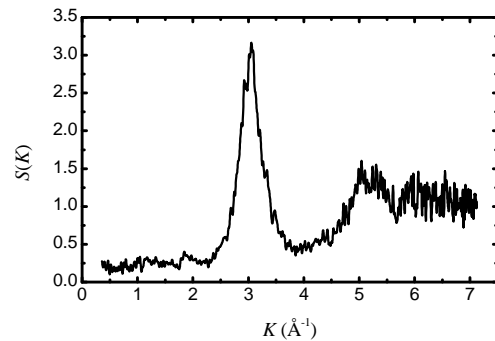


FIG. 1: Experimental total structure factor for  $\alpha$ -Co<sub>57</sub>Ti<sub>43</sub>.

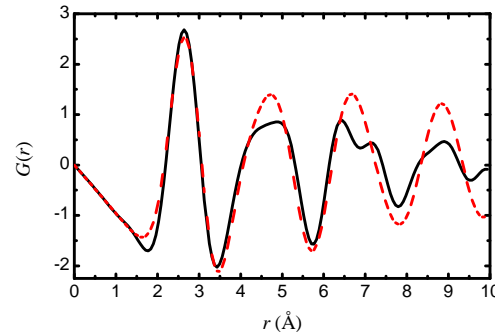


FIG. 2: Experimental (solid line) and AHS (dashed line)  $G(r)$  functions for  $\alpha$ -Co<sub>57</sub>Ti<sub>43</sub>.

ing the spherical waves method [24] and FEFF software. Figure 5 shows the experimental and the fitting results for the Fourier-filtered first shells on Co and Ti edges. The high quality of the fit on Ti edge is evidenced on the inset at fig. 5.b, which shows the high- $k$  EXAFS data on this edge together with its simulation. Structural parameters extracted from the fits are listed in table I. As it can be seen in this table, on Co edge one Co-Co shell and one Co-Ti shell were considered in the first shell in order to find a good fit, whereas on Ti edge one Ti-Ti shell and two Ti-Ti subshells were needed. We started the fit-

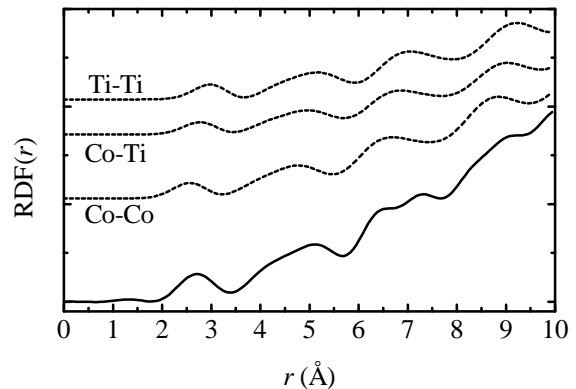


FIG. 3: Experimental RDF( $r$ ) (solid line) and partial RDF $_{ij}^{\text{AHS}}(r)$  (dashed lines) functions for  $\alpha$ -Co<sub>57</sub>Ti<sub>43</sub>.

TABLE I: Structural data determined for  $a$ -Co<sub>57</sub>Ti<sub>43</sub>.

EXAFS					
	Co K-edge		Ti K-edge		
Bond Type	Co-Co	Co-Ti	Ti-Co	Ti-Ti <sup>a</sup>	
$N$	6.0	6.0	7.9	1.9	3.0
$r$ (Å)	2.50	2.52	2.52	2.81	3.08
$\sigma^2$ (Å <sup>2</sup> ×10 <sup>-2</sup> )	1.45	4.57	4.57	1.46	1.29
AHS-RDF					
Bond Type	Co-Co	Co-Ti	Ti-Co	Ti-Ti	
$N$	6.5	5.5	7.3	4.0	
$r$ (Å)	2.49	2.75	2.75	3.17	
bcc-Co <sub>2</sub> Ti [21]					
Bond Type	Co-Co	Co-Ti	Ti-Co	Ti-Ti	
$N$	6	6	12	4	
$r$ (Å)	2.37	2.77	2.77	2.90	

(<sup>1</sup>) There are 4.9 Ti-Ti pairs at  $\langle r \rangle = 2.96$  Å.

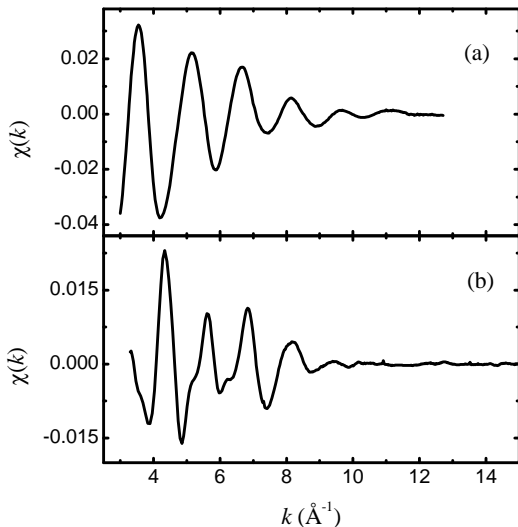


FIG. 4: Experimental EXAFS spectra: (a) Co K edge and (b) Ti K edge.

ting procedure using one shell for all pairs. This choice did not produce a good quality fit of Fourier-filtered first shells on the Ti edge. Besides that, the well-known relations  $c_i N_{ij} = c_j N_{ji}$ ,  $r_{ij} = r_{ji}$  and  $\sigma_{ij} = \sigma_{ji}$ , where  $c_i$  is the concentration of atoms of type  $i$ ,  $N_{ij}$  is the number of  $j$  atoms located at a distance  $r_{ij}$  around an  $i$  atom and  $\sigma_{ij}$  is the half-width of the Gaussian, were not verified in fitting EXAFS data. By considering two Ti-Ti subshells the quality of the fit on the Ti edge was much improved (see fig. 5). Moreover, the relations above were satisfied. It should be noted that Nyquist criterion as defined in ref. [25] is also satisfied even with two Ti-Ti subshells due to the large  $k$ -data range.

Comparing EXAFS and AHS-RDF results it can be seen that concerning coordination numbers they show a

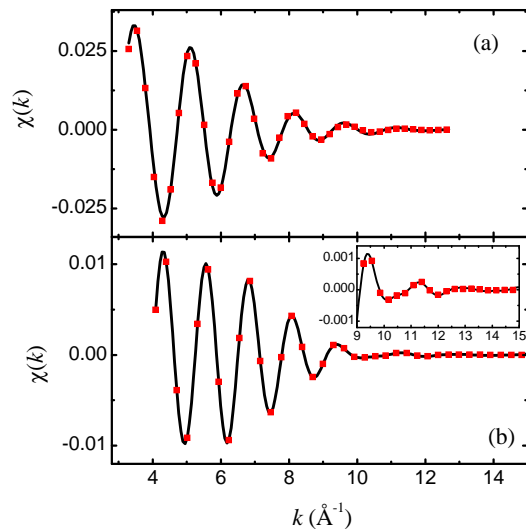


FIG. 5: Fourier-filtered first shell (full line) and its simulation (squares) on (a) Co K edge, (b) Ti K edge. The inset at (b) shows the high- $k$  EXAFS data and its simulation.

good agreement, mainly if the difficulties in finding data about Ti-Ti pairs by the AHS-RDF analysis mentioned above are considered. In addition, coordination numbers determined by EXAFS have an error of about 1 atom for this kind of alloys. However, except for the Co-Co interatomic distance, AHS-RDF results overestimate distance values, which could be explained by the considerations made in the definition of the AHS model. This decrease in the distances is not unexpected because, according to Hausleitner and Hafner [26], which investigated several amorphous alloys formed by transition metals (TM-Ti) using molecular dynamics simulations, obtaining structure factors, coordination numbers and interatomic distances, if the components of an alloy have a large difference in the number of  $d$  electrons there is a pronounced non-additivity of the pair interactions and a strong interaction between unlike atoms, thus decreasing the distance between chemically different atoms. The shortening effect is even stronger in  $a$ -Ni<sub>60</sub>Ti<sub>40</sub> [3] produced by MA. This alloy has 8.8 Ni-Ni pairs at  $\langle r \rangle = 2.58$  Å, 5.2 Ni-Ti pairs at  $\langle r \rangle = 2.55$  Å and 5.5 Ti-Ti pairs at  $\langle r \rangle = 2.90$  Å, and in this case Ni-Ti pairs are even shorter than Ni-Ni pairs. Comparing  $a$ -Ni<sub>60</sub>Ti<sub>40</sub> and  $a$ -Co<sub>57</sub>Ti<sub>43</sub> it can be seen that structural data are similar, the main difference being the number of TM-TM pairs (TM = Ni or Co), which is larger in the first alloy probably because of its stronger CSRO. In addition, the shortening effect was also found by Fukunaga *et al.* in  $a$ -Ni<sub>40</sub>Ti<sub>60</sub> produced by melt-quenching [27], and recently we have also seen it in  $a$ -Cu<sub>64</sub>Ti<sub>36</sub> produced by MA, whose data will be published elsewhere (we have chosen not to compare with Fe<sub>60</sub>Ti<sub>40</sub> [9] because this alloy is not completely amorphous). It is interesting to note that the local structure of  $a$ -Co<sub>57</sub>Ti<sub>43</sub> shows some differences when compared to that found in the bcc-Co<sub>2</sub>Ti compound. The composi-

tional difference may explain the disagreement between Co-Ti coordination numbers, but there is an important reduction in the Co-Ti distance in the amorphous alloy, whereas Co-Co and Ti-Ti distances increase. These features usually are attributed to the preparation technique, that introduces many defects and vacancies in the alloy, and they have also been reported for other alloys produced by MA [3, 28, 29].

In order to estimate the CSRO in the alloy we used the generalized Warren parameter  $\alpha_W$  given by [30]

$$\alpha_W = 1 - \frac{N_{12}}{c_2 N} = 1 - \frac{N_{21}}{c_1 N},$$

where  $N_{ij}$  are the coordination numbers and  $N_i = \sum_j N_{ij}$  and  $N = c_1 N_2 + c_2 N_1$ . The  $\alpha_W$  parameter is null for a random distribution. If there is a preference for forming unlike pairs in the alloy, it becomes negative. Otherwise, it is positive if homopolar pairs are preferred. Here, using the coordination numbers given in table I, we found  $\alpha_W^{\text{EXAFS}} = -0.117$  and  $\alpha_W^{\text{AHS}} = -0.103$ . Since the values of  $\alpha_W$  are negative and small, they indicate a weak CSRO in the alloy, in agreement with the results above.

## VI. CONCLUSION

An amorphous  $\text{Co}_{57}\text{Ti}_{43}$  alloy was produced by Mechanical Alloying technique and its local atomic structure

was obtained from EXAFS analysis, which furnished coordination numbers and interatomic distances between first neighbors. The results found were compared with those determined by using an additive hard sphere model combined with an  $\text{RDF}(r)$  deconvolution process. Concerning coordination numbers, there is a good agreement between EXAFS and AHS-RDF data. However, AHS-RDF furnishes interatomic distances for Co-Ti and Ti-Ti pairs too large when compared to EXAFS results, which could be attributed to the way the AHS model is defined. In addition, we have also seen the decrease in Co-Ti distance as proposed by Hausleitner and Hafner [26] for TM-Ti alloys. There is a small CSRO in the alloy, and a preference for forming unlike pairs. The local structure of  $\alpha\text{-Co}_{57}\text{Ti}_{43}$  is not much different from that found in  $\alpha\text{-Ni}_{60}\text{Ti}_{40}$  except for the number of TM-TM pairs (TM = Ni or Co), which is larger in the second alloy. However,  $\alpha\text{-Co}_{57}\text{Ti}_{43}$  has a local structure different from that found in  $\text{bcc-Co}_2\text{Ti}$  compound, as seen in other alloys produced by MA [3, 28, 29].

## Acknowledgments

We thank CNPq, CAPES and LNILS (proposal no XAS 799/01) for financial support.

- 
- [1] C. Suryanarayana, *Prog. Mater. Sci.* **46**, 1 (2001).
  - [2] K. D. Machado, J. C. de Lima, C. E. M. Campos, T. A. Grandi, and A. A. M. Gasperini, *Sol. State Commun.* **127**, 477 (2003).
  - [3] K. D. Machado, J. C. de Lima, C. E. M. de Campos, T. A. Grandi, and D. M. Trichês, *Phys. Rev. B* **66**, 094205 (2002).
  - [4] B. P. Dolgin, M. A. Vanek, T. McGory, and D. J. Ham, *J. Non-Cryst. Sol.* **87**, 281 (1986).
  - [5] E. Hellstern and L. Schultz, *Mater. Sci. and Eng.* **93**, 213 (1987).
  - [6] H. Kimura, F. Takada, and W.-N. M. W.-N., *Mat. Sci. Eng.* **97**, 125 (1988).
  - [7] A. R. Yavari, P. J. Desré, and T. Benameur, *Phys. Rev. Lett.* **68**, 2235 (1992).
  - [8] M. Abbate, W. H. Schreiner, T. A. Grandi, and J. C. de Lima, *J. Phys.: Cond. Matter* **13**, 5723 (2001).
  - [9] J. C. D. Lima, K. D. Machado, V. Drago, T. A. Grandi, C. E. M. Campos, and D. M. Trichês, *J. Non-Cryst. Solids* **318**, 121 (2003).
  - [10] M. Naka, N. S. Kazama, H. Fujimori, and T. Masumoto, *Proc. 5<sup>th</sup> Int. Conf. Rapidly Quenched Metals* (Wurzberg, 1984).
  - [11] M. Nose, K. Esashi, J. Kanehira, S. Ohnuma, K. Shirakawa, and T. Masumoto, *Proc. 4<sup>th</sup> Int. Conf. Rapidly Quenched Metals* (Wurzberg, 1982).
  - [12] B. K. Teo and D. C. Joy, *EXAFS Spectroscopy, Techniques and Applications* (Plenum, New York, 1981).
  - [13] P. A. Lee, P. Citrin, P. Eisenberger, and B. Kincaid, *Rev. Mod. Phys.* **53**, 769 (1981).
  - [14] T. M. Hayes and J. B. Boyce, *Solid State Physics* (Academic Press, New York, 1982), vol. 37, p. 173.
  - [15] J. J. Rehr and R. C. Albers, *Rev. Mod. Phys.* **72**, 621 (2000).
  - [16] D. C. Koningsberger and R. Prins, *X-ray Absorption* (Wiley, New York, 1988).
  - [17] T. E. Faber and J. M. Ziman, *Philos. Mag.* **11**, 153 (1965).
  - [18] J. D. Weeks, *Phil. Mag.* **35**, 1345 (1977).
  - [19] Y. Waseda, *The Structure of Non-Crystalline Materials (Liquid and Amorphous Solids)* (McGraw-Hill, New York, 1980).
  - [20] C. N. J. Wagner, *Liquid Metals* (S. Z. Beer, Marcel Dekker, New York, 1972).
  - [21] TAPP, version 2.2 (1990), E. S. Microwave, Inc., 2234 Wade Court, Hamilton, OH 45013.
  - [22] T. Ressler, *J. Phys.* **7**, C2 (1997).
  - [23] E. A. Stern, D. E. Sayers, and F. W. Lytle, *Phys. Rev. B* **11**, 4836 (1975).
  - [24] J. J. Rehr, *J. Am. Chem. Soc.* **113**, 5135 (1991).
  - [25] E. A. Stern, *Phys. Rev. B* **48**, 9825 (1993).
  - [26] C. Hausleitner and J. Hafner, *Phys. Rev. B* **45**, 128

- (1992).
- [27] T. Fukunaga, N. Watanabe, and K. Suzuki, *J. Non-Cryst. Solids* **61** & **62**, 343 (1984).
- [28] K. D. Machado, J. C. de Lima, C. E. M. Campos, T. A. Grandi, and P. S. Pizani, *J. Chem. Phys.* **120**, 329 (2004).
- [29] K. D. Machado, P. Jóvári, J. C. de Lima, C. E. M. Campos, and T. A. Grandi, *J. Phys.: Condens. Matter* **16**, 581 (2004).
- [30] D. Gazzillo, G. Pastore, and S. Enzo, *J. Phys.: Condens. Matter.* **1**, 3469 (1989).